

# Face-selective neurons in the vicinity of the human fusiform face area

Vadim Axelrod, PhD, Camille Rozier, PhD, Tal Seidel Malkinson, PhD, Katia Lehongre, PhD, Claude Adam, MD, PhD, Virginie Lambrecq, MD, PhD, Vincent Navarro, MD, PhD, and Lionel Naccache, MD, PhD

*Neurology*® 2019;92:197-198. doi:10.1212/WNL.0000000000006806

## Correspondence

Dr. Axelrod  
vadim.axelrod@gmail.com

Face perception is thought to be mediated by neural activity in the occipital and posterior temporal cortex.<sup>1,2</sup> However, the face-selective neurons at the cellular level in these areas in humans have never been demonstrated. We had a rare opportunity to record intracranial multi-unit activity in an epilepsy patient near the fusiform face area<sup>2</sup> (figure 1A). We identified 2 units with highly face-selective response to static images of familiar (famous) and unfamiliar faces (figure 1B and video 1; figure e-1a, doi.org/10.5061/dryad.81t0fq1) as well as to human and animal faces that appeared in a movie (figure 1C, video 1, figure e-1b).

## MORE ONLINE

### Video

## Author contributions

V. Axelrod: conceiving the study, designing and preparing the experiments, analyzing the data, writing, editing and revising the manuscript. C. Rozier: data acquisition. T.S. Malkinson: data acquisition, editing the manuscript. K. Lehongre: responsibility for intracranial recording infrastructure, editing the manuscript. C. Adam: responsibility for intracranial recording infrastructure. V. Lambrecq: responsibility for intracranial recording infrastructure, editing the manuscript. V. Navarro: responsibility for intracranial recording infrastructure, editing the manuscript. L. Naccache: conceiving the study, supervising the project, editing the manuscript.

## Acknowledgment

The authors thank the patient for participating in this study, Leila Reddy for advice on using the wave\_clus tool, and Roy Export SAS for permission to use material from *The Circus*.

## Study funding

This study was supported by an Alon Fellowship for outstanding young faculty members by the Israeli Council for Higher Education (V.A.), Israel Science Foundation (S7/15) and Marie Skłodowska-Curie (702577) fellowships (T.S.M.), and the program “Investissements d’avenir” ANR-10-IAIHU-06 and the ICM-OCIRP.

## Disclosure

The authors report no disclosures relevant to the manuscript. Go to [Neurology.org/N](http://Neurology.org/N) for full disclosures.

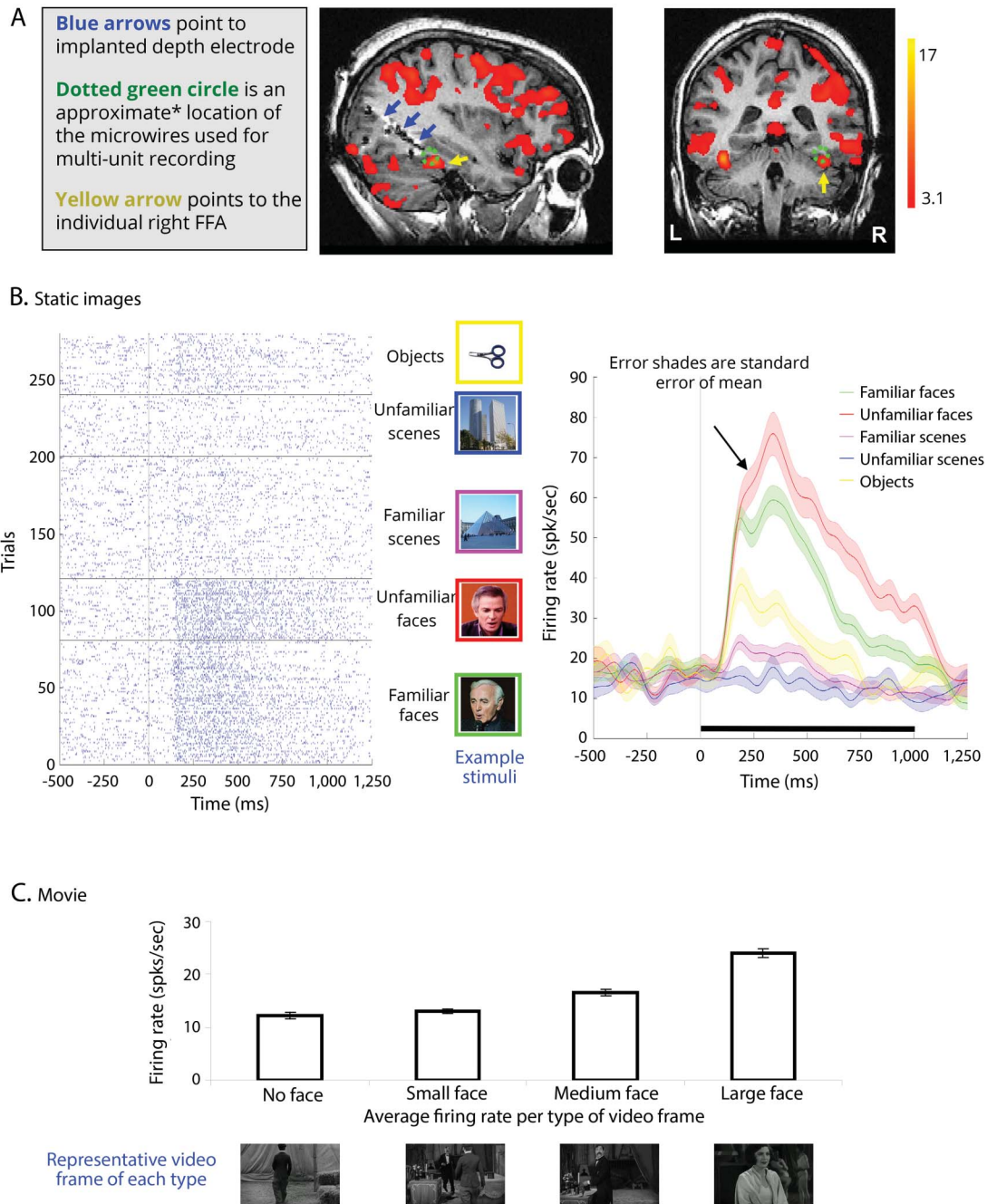
## References

1. Bentin S, Allison T, Puce A, Perez E, McCarthy G. Electrophysiological studies of face perception in humans. *J Cogn Neurosci* 1996;8:551–565.
2. Kanwisher N, Yovel G. The fusiform face area: a cortical region specialized for the perception of faces. *Philos Trans R Soc B Biol Sci* 2006;361:2109–2128.

From The Gonda Multidisciplinary Brain Research Center (V.A.), Bar Ilan University, Ramat Gan, Israel; Institut National de la Santé et de la Recherche Médicale Unité 1127 (C.R., T.S.M., K.L., V.L., V.N., L.N.), Centre National de la Recherche Scientifique Unité Mixte de Recherche (UMR) 7225, Sorbonne Université, Université Pierre-et-Marie-Curie Univ Paris 06 UMR S 1127, Institut du Cerveau et de la Moelle Épineuse; Centre de NeuroImagerie de Recherche-CENIR (K.L.), Institute of Brain and Spine, UMRS 1127, CNRS UMR 7225, Pitié-Salpêtrière Hospital; Epilepsy Unit and Neurophysiology Department (C.A., V.L., V.N.), AP-HP, GH Pitié-Salpêtrière-Charles Foix; and Departments of Neurology and Neurophysiology (L.N.), AP-HP, Groupe Hospitalier Pitié-Salpêtrière, Paris, France.

Go to [Neurology.org/N](http://Neurology.org/N) for full disclosures.

**Figure** Recording location and the results of unit 1



1(A) Anatomic image with overlaid individual functional MRI activations (contrast: face > objects;  $p < 0.001$ , uncorrected). (B) Experiment with static images: left is a raster plot (horizontal gray lines separate the different conditions); right is across trials' mean instantaneous firing rate per condition. Note the high face-selectivity in both face conditions. Credits for images: unfamiliar scene: Avishai Taicher (CC BY 2.5), familiar scene: user: ewrfpiuqwnpiqfnpwi (CC BY 2.5), unfamiliar face: Moshe Sinai, familiar face: shutterstock.com. (C) Movie experiment (6-minute fragment of *The Circus* silent film). Movie frames ( $n = 1,800$ ) were binned into 4 different types of frames of the movie: large, medium, small, and no faces. Note the higher average firing rate for frames with large faces. Error bars denote the standard error of mean. \*Human electrophysiology does not permit us to establish unequivocally whether the units were within the boundaries of the fusiform face area (FFA; e-Methods, doi.org/10.5061/dryad.81t0fq1). Permission to reproduce material from *The Circus* movie: Charles Chaplin, *The Circus*; Copyright Roy Export SAS; all rights reserved (office@charliechaplin.com).

## Contents

Supplementary Methods .....	2
Supplementary Results .....	9
Supplementary Figure.....	12
Supplementary References.....	13

## Supplementary Methods

### Participants

The patient was a 26-year-old, right-handed French-speaking female who had no cognitive impairments (see next paragraph for detailed neuropsychological history of the patient). For clinical purposes of epilepsy seizure monitoring, the patient was implanted with depth electrodes. The electrodes were implanted in the right occipital and temporal lobes. The location of the electrodes was determined solely by clinical criteria. There was no epileptic activity in the location where the electrode reported in this paper was implanted (right posterior fusiform gyrus; see below). The study was conducted during the patient's hospitalization in the Epilepsy ward. The clinical setup was the same as in the previous intracranial studies conducted in Pitié-Salpêtrière Hospital<sup>1-4</sup>. The study was approved by the local ethics committee (CPP Paris VI, INSERM C11-16) and was conducted according to ethical approval and guidelines. The patient gave written informed consent to participate in the study.

The patient developed non-lesional focal epilepsy at the age of 22. The epilepsy was rapidly becoming drug-resistant, and seizures were occurring several times a month, with frequent secondarily generalized tonic-clonic seizures. EEG, functional imagery, and clinical features were suggestive of occipital lobe epilepsy. Analysis of sEEG recordings revealed a bifocal epilepsy with a major epileptogenic focus contained in the external part of the right occipital pole. The patient had normal early neurological and psychomotor development, no family and personal history of epilepsy, and no precipitating factors. The patient had 18 years of education (i.e., higher education) and was pursuing an internship as a medical doctor at the time of the study. The patient had normal cognitive abilities and no memory impairments. The patient had an IQ = 92 (verbal IQ = 96, performance IQ = 90). Normal cognitive abilities were also reflected by her high behavioral performance in our experiments (see Results).

### Recording setup

Stereotactic EEG (sEEG) was conducted using depth platinum macro-electrodes (AdTech, Wisconsin) of the Behnke-Fried type<sup>5</sup>. The patient was implanted with eight macro electrodes. The only relevant electrode for the present report was implanted in the right posterior fusiform gyrus (Fig. 1A). Eight platinum-iridium microwires protruded about 5 mm beyond the macro-electrode tip of this electrode. This paper focuses only on microwire recordings. The signal was recorded using the Atlas recording system (Neuralynx Inc., Tucson, AZ). The microwire recording sampling rate was 32 kHz and online band-pass filter was 0.1–4000 Hz. As reference, one of the eight microwires with lowest MUA and local field potential (LFP) activity is used. The same multi-unit recording setup was used previously in Pitié-Salpêtrière Hospital<sup>1</sup>. The data presented in the paper are from four contacts for which spiking activity could be detected (sufficient signal-to-noise ratio).

## Intracranial experiments

### Experimental setup

The experiment was conducted in a hospital ward where the patient stayed (quiet room, no other people). Stimuli were projected on a Dell Precision M4600 laptop (15.6 inch display, 1366 × 768 resolution). The patient was sitting approximately 50 cm from the monitor. The experiments were run on MATLAB (R2012a) using Psychtoolbox 3<sup>6</sup>.

### Experiment 1:

The stimuli were color images of faces, objects, and scenes that were collected from various Internet sources (see examples in Fig. 1B). Face images included faces of famous French individuals (e.g., politicians, actors) and faces of famous non-French individuals (e.g., Israeli politicians, actors). Two conditions of French and non-French individuals were matched with regard to the number of female / male identities, age of the identities and professions of the identities). Scene images were well-known Paris sites and sites outside France. Two types of scene images were matched with regard to buildings types (e.g., new and historical buildings) and lighting (i.e., number of photos taken during the day and night). For each of five conditions (i.e., familiar and unfamiliar faces, familiar

and unfamiliar scenes, and objects) there were 10 identities (i.e., face personalities, scene locations, and object types). Each identity was represented by 4 different exemplars (e.g., 4 different pictures of Nicolas Sarkozy). The size of the stimuli was about 11° visual angle. Stimuli from unfamiliar faces, unfamiliar scenes and objects conditions were repeated once per experiment (i.e., 40 trials per condition). Stimuli from familiar faces and familiar scenes conditions were repeated twice per experiment (i.e., 80 trials per condition). This design permits to test selectivity for category and for identity. The order of the conditions was pseudo-random. The stimuli duration and fixation before the stimulus were 1 second and 1.2 seconds, respectively. The design and timing parameters were chosen based on previous MUA studies in humans <sup>7, 8</sup>. For each stimulus (i.e., a trial) the patient had to indicate whether the stimulus was familiar or unfamiliar (pressing "1" or "2" on the computer keyboard). The next trial appeared only after the patient responded to the previous one. Before the main session of the experiment, the patient took part in a short training session that included 10 trials. The training stimuli were not used in the main session.

#### Experiment 2:

The experiment consisted of a fragment (6 min) from "The Circus" silent movie (release year: 1928; director and principal role: Charlie Chaplin). The movie was shown with sound (background music). The size of the movie frame was 19.8° (horizontal) and 15.2° (vertical). The patient was instructed to watch the movie (no active task).

#### MUA data analysis

Data analysis was conducted in MATLAB (R2009B). Spike detection and spike sorting were conducted using a standard pipeline for analyzing human MUA <sup>7-9</sup>. Prior to the MUA analysis we visually inspected the LFP signals of the microwires to ensure that there was no epileptic activity. Spike detection and spike sorting were performed using wave\_clus toolbox <sup>10</sup>. The toolbox applies a band-pass filter (300-3000 Hz), while the amplitude threshold for spike detection is determined automatically. Spike-sorting is done by first extracting the relevant features of spike waveforms using wavelet transform and then by performing super-paramagnetic clustering <sup>11</sup>. In any of the units, the average

of the cluster (i.e., cluster shape average) did not exceed 50  $\mu\text{V}$  (see Fig. 1A); therefore, the units were classified as MUA<sup>7,8</sup>.

### Experiment 1

The data were epoched to conditions (baseline: 500 ms, trial period: 1250 ms). The instantaneous firing rate was calculated by convolving a Gaussian kernel with spike trains of individual trials. The data were then normalized using the z-score MATLAB function<sup>9</sup>. MUA studies in humans usually focus on late activity (e.g., 200–300 ms+)<sup>7,9</sup>, so they used relatively large Gaussian kernel values (e.g., FWHM=100 ms). While this Gaussian kernel value is suitable for the later activity, it is less ideal for the early evoked response (i.e., it distorts a precise timing). Given that in our study we were interested in both early and later activity, in our statistical analyses we used two different Gaussian kernels, depending on the time period. To achieve higher time precision for the evoked period of 0–200 ms, a Gaussian kernel of FWHM=30 ms was used [for similar value, see ref.<sup>12</sup>]. For the remaining period of 201–1000 ms, a Gaussian kernel of FWHM=80 ms was used. For all the plots, the FWHM=80 ms Gaussian kernel was used.

Statistical tests were conducted after subtracting the baseline mean value for each trial (i.e., baseline correction). The statistical significance (i.e., one-sample t-test vs. baseline, two sample t-tests between conditions and one-way ANOVA between conditions) was evaluated using a cluster-based permutation approach<sup>13</sup> and implemented using the logic used by Kornblith and colleagues<sup>9</sup>. The tests were conducted between trials and within the unit. For each point in time, the t-value (for t-tests) or F-value (for one-way ANOVA) are calculated. The clusters of contiguous points in time for which the significance is above  $p < 0.01$  were found, and the sum of the t-values or F-values was calculated. The labels were randomly reshuffled 1000 times, and for each reshuffled round we find a cluster with a maximal sum of t-values or F-values. Distribution of maximal sums of t-values or F-values of reshuffled data is used to establish how significant (i.e., p-value) is the result obtained using the original (non-reshuffled) data. The t-tests were two-tailed.

### Experiment 2

The instantaneous firing rate was calculated by convolving Gaussian kernel (FWHM=80 ms) with a spike train (duration: 6 minutes). The data were then normalized (z-score). To conduct a quantitative analysis of face-selectivity across the whole movie fragment, we examined the correspondence between the content of the frames and the neural activity. To this end, we binned the movie frames to four categories: large face (larger than 2.5° of visual angle; 204 frames), medium face (from 1.25° to 2.5°; 678 frames), small face (smaller than 1.25°; 443 frames) and no face (475 frames). Example frames are shown in Fig. 1C. In cases where more than one face appeared in the frame, the largest face was considered. Classification of the frames was done without looking at the neural data to prevent any potential bias. The analysis was conducted using a time window of 200 ms [for similar time window in MUA analysis, see ref<sup>14</sup>]. The firing rate within the window was averaged. For the control analyses, we tested time windows of 100 ms and 500 ms, and the results were qualitatively similar. Note that in order to avoid introducing any potential bias, in our analysis we deliberately made as few assumptions as possible. For example, we did not exclude any frames, in particular the frames in which the faces were potentially not attended. The fact that even using our simplistic approach it was possible to observe a substantial difference between conditions, suggests that the face-selective units are indeed sensitive to faces in the movie.

#### MRI anatomical clinical scanning

The MRI anatomical scan (T1) in Fig. 1A was acquired for clinical purposes after the implantations of the electrodes (i.e., the electrodes were inside the brain). The image was acquired using a 1.5 T GE Optima MR450w scanner (in-plane resolution=1x1 mm, slice thickness=1.3 mm, acquisition matrix of 256x256, number of slices=134, TE=4.28 ms, repetition time [TR]=10.56 ms, Inversion Time=450 ms). The macro-electrodes are clearly visible on this T1 image (Fig. 1A, blue arrows). The microwires, however, cannot be seen on the MRI image. On the CT scan that was also acquired, the microwires were more visible, but still only partially and not clearly enough to be confident regarding their precise location. Therefore, similar to other MUA recording studies in humans<sup>15</sup>, we define only the approximate location of the microwires (Fig. 1A, dotted green circle).

## Functional MRI experiment

The fMRI experiment was conducted after the electrodes had been already removed (several months after the intracranial implantation). The data were acquired by a 3T Verio MRI scanner (Siemens, Erlangen, Germany). Stimuli were back-projected with head mounted mirror. Two-button MRI-compatible response box (Current Designs, Philadelphia, USA) was used to acquire behavioral responses. An echo planar imaging (EPI) sequence was used for acquiring functional data (T2\*- weighted images, TR = 1450 ms, echo time TE = 25 ms, flip angle [FA] = 71°, acquisition matrix of 110×110, number of slices=72, 2x2x2 mm isomorphic voxel, whole brain coverage, multiband sequence). The anatomical (T1) image was acquired using MPRAGE pulse sequence (0.8x0.8x0.8 mm isomorphic voxel, acquisition matrix of 320×320, number of slices=256, TR = 2400 ms, TE = 2.05 ms, Inversion Time=1000 ms).

The experiment was a standard visual functional localizer that was used in many previous studies including our own <sup>16-20</sup>. The experiment was run on MATLAB (R2012a) using Psychtoolbox 3 <sup>6</sup>. The experiment included stimuli of four categories: faces, scenes, objects, and scrambled objects (i.e., pixel-scrambled versions of object images). All the images were unfamiliar to the patient. The size of the stimuli was about 11°. For the present study, only the results of "faces" and "objects" conditions are reported (note that all the conditions were included in the GLM model). Block design was used for the experiment (block duration: 15 seconds). Each block consisted of 15 stimuli (stimulus duration and interstimulus interval (ISI) were 0.3 seconds and 0.7 seconds, respectively). Four blocks for each condition (pseudo-random order) were followed by a block with fixation cross (15 seconds duration). The session included 5 repetitions of each condition (i.e., 5 blocks of faces, 5 blocks of objects, etc). The task was "1-back": to press any button on a response box when the same image is repeated one after another. The total duration of a session was 6 minutes and 35 seconds (including 10 seconds of the fixation cross at the beginning and 10 seconds of the fixation cross at the end). The experiment included 5 sessions.

The analysis presented in the paper has been conducted using an FSL package, version 5<sup>21</sup>. For validation, we repeated the analysis using an SPM 5 package (Wellcome Trust Centre for Neuroimaging, London, UK; <http://www.fil.ion.ucl.ac.uk>) and the results were very similar. Standard preprocessing and analysis pipeline was run using a FEAT tool. Preprocessing included motion correction using MCFLIRT, brain extraction using BET, high-pass temporal filtering, and smoothing using full width at half maximum (FWHM) of 5 mm. The analysis was conducted in native space (without normalization), so the functional data were co-registered to the T1 image scanned with the implanted electrodes. The quality of the co-registration was validated by visual inspection. The GLM model (gamma hemodynamic response function) was estimated with five regressors (four conditions and the fixation blocks). The faces > objects contrast was defined at the first-level analysis. Higher-level analysis has been conducted across sessions. The results shown in Fig. 1A are the functional activations (faces > objects contrast,  $p < 0.001$  uncorrected) overlaid on the T1 image with implanted electrodes. Note that  $p < 0.001$  uncorrected threshold is standard practice for defining individual face-selective activations<sup>22, 23</sup>. We can see that the FFA (Fig. 1A, yellow arrows) was localized in its typical location<sup>22</sup>. As we explained above, we could not establish unequivocally the location of the microwires. Critically, we can see that the microwires were at least proximate to the FFA or even within the FFA.

## Supplementary Results

### Static images experiment (Experiment 1)

The experiment included images of faces, scenes, and objects (see example stimuli in Fig. 1A and Video 1). Faces and scenes were subdivided into those familiar to the patient (i.e., French famous people and scenes) and unfamiliar (i.e., non-French famous people and scenes). The task was to respond whether the stimulus was familiar or not. The percentage of correct behavioral responses per category was as follows: familiar faces=100%, unfamiliar faces=95%, familiar scenes=95%, unfamiliar scenes=0.22%, and objects=100%. The reason for low performance in the "unfamiliar scenes" category was that the patient thought that the task required an answer of "familiar" even when an unfamiliar scene resembled some familiar scene. Most critically, the results show that with regard to face recognition, the patient was almost perfect.

At the neural level, the firing of unit 1 strongly increased for faces (Fig. 1B and Video 1). Modulation versus baseline was about 400%, which is remarkable compared to the 0.5%–1.5% usually found in fMRI studies<sup>43, 49-52</sup>. Statistically, the firing rate for faces (collapsed across familiarity) was above baseline from 126 to 919 ms ( $p < 0.001$ , two-tail nonparametric cluster-based permutations<sup>37</sup>; see Methods). Above baseline increase in firing rate has been also found for objects (145:463 ms;  $p < 0.001$ ) and to a very minimal extent for scenes (151:194 ms;  $p = 0.003$ ). One-way ANOVA with faces, scenes, and objects as factors, conducted for baseline corrected data, revealed a significant main effect [129:1000 ms,  $p < 0.001$ , nonparametric cluster-based permutation<sup>37</sup>]. Post-hoc two-sample two-tailed t-tests revealed higher firing rates for faces than for scenes (125:1000 ms,  $p < 0.001$ ), higher for faces than for objects (142:1000 ms,  $p < 0.001$ ), and higher for objects than for scenes (146:407 ms),  $p = 0.001$ ). Later in time, a higher firing rate was elicited by unfamiliar compared to familiar faces (251:379,  $p = 0.028$ ; 510:927 ms,  $p < 0.001$ ).

Strong face-selectivity was also found in unit 2 (Supplementary Fig. 1A). An above baseline increase of firing rate has been found for faces (122:892 ms,  $p < 0.001$ ), scenes

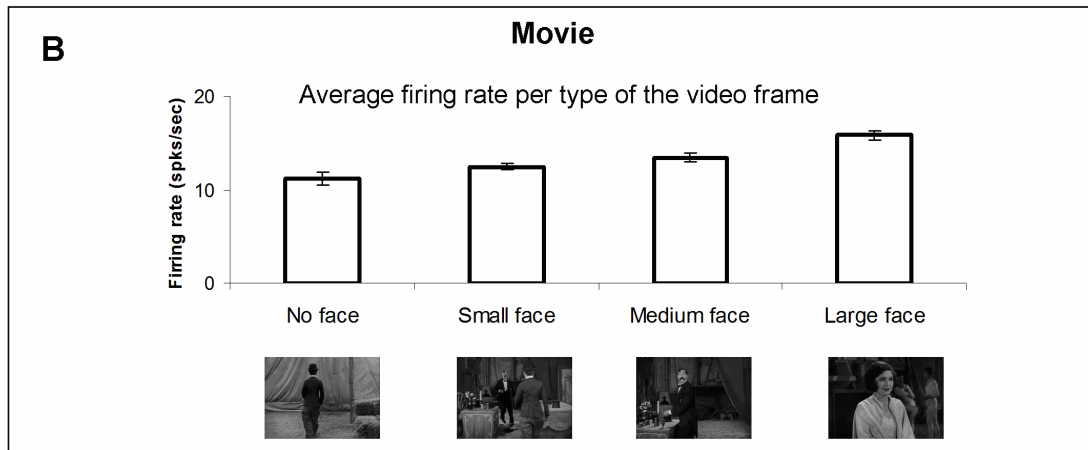
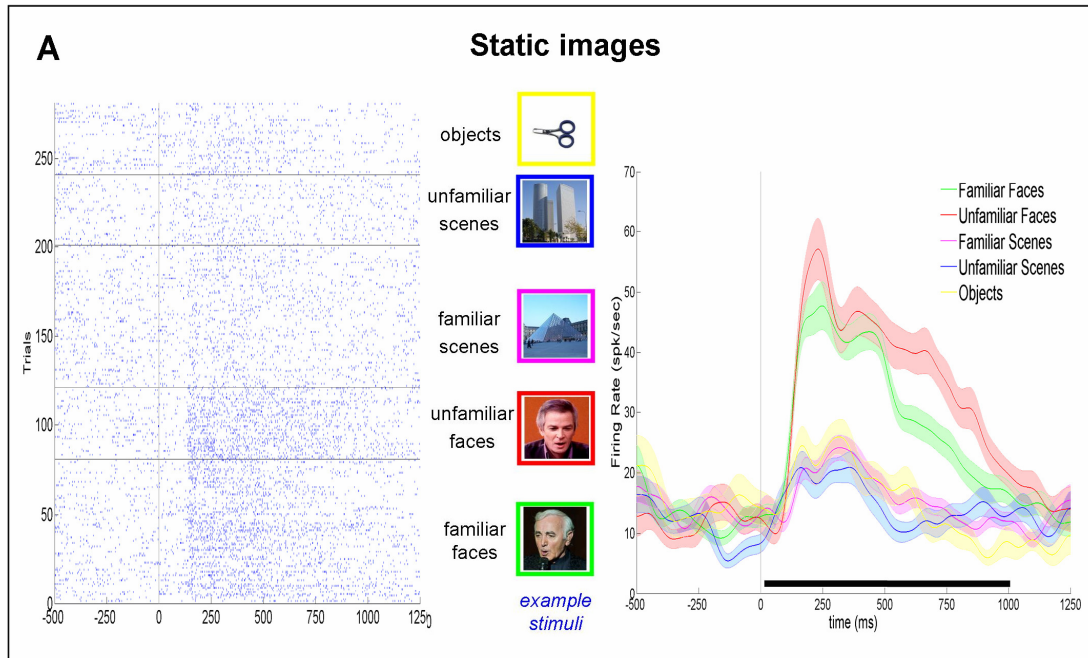
(141:470 ms,  $p < 0.001$ ), and objects (145:179 ms,  $p = 0.011$ ; 260:362 ms,  $p < 0.019$ ). One-way ANOVA with faces, scenes, and objects as factors revealed a significant main effect [126:1000 ms,  $p < 0.001$ ). The post-hoc two sample t-tests revealed higher firing rates for faces than for scenes (123:1000 ms,  $p < 0.001$ ) and for faces compared to objects (132:1000 ms,  $p < 0.001$ ). A small difference was also found between objects and scenes (874:963 ms,  $p = 0.036$ ). Higher firing rates have been elicited by unfamiliar compared to familiar faces (540:744 ms,  $p = 0.007$ ).

### Movie experiment (Experiment 2)

Experiment 1 identified units that were selective to static images of faces. In experiment 2 we asked whether this face-selectivity phenomenon can be found for dynamic faces, such as the faces that appear in a movie – a more natural stimulation compared to static images<sup>9, 53, 54</sup>. To this end, in Experiment 2 the patient was shown a movie fragment of 6 minutes ("The Circus", a silent film). Qualitatively, the appearance of faces (or more visible faces) modulated the firing rate. Modulation was found not only for human but also for animal faces (Video 1). For quantitative analysis, the frames of the movie were divided into four categories: frames with large, medium, small, and no face (see Methods). We found that the frames with larger (and more visible) faces elicited higher firing rates compared to smaller faces or frames without a face (Fig. 1C). Statistically, a one-way ANOVA with the four frame types as factors revealed a highly significant main effect [ $F(3,1796) = 47.81$ ,  $p < 0.001$ ]. A post-hoc t-test revealed higher firing rates for "large face" compared to all other types of frames ( $p < 0.001$ ), as well as higher firing rates for "medium face" compared to "small face" and "no face" types of frame ( $p < 0.001$ ). Note that the patient watched a movie in a completely natural way, without any instructions. It is possible, therefore, that not all faces that appeared during the movie were noticed or/and attended. Thus, the fact that even using a simplistic analytical approach (i.e., binning the frames by face size) it was possible to observe a substantial difference between conditions, suggests that the face-selective units are indeed sensitive to faces in the movie.

The effects in face-selective unit 2 were similar (albeit smaller) to those found in face-selective unit 1 (Supplementary Fig. 2B). One-way ANOVA with the four frame types as factors revealed a highly significant main effect [ $F(3,1796)=9.7$ ,  $p<0.001$ ]. The post-hoc t-test revealed higher firing rates for "large face" compared to "small face" ( $p<0.001$ ). In addition, the firing rate during "medium face" was higher than in "no face" [ $t(1292)=2.56$ ,  $p=0.01$ ].

## Supplementary Figure



**Supplementary Figure 1.** Results of face-selective unit 2. **(A)** Experiment with static images: left is a raster plot (horizontal grey lines separate the different conditions); right is across trials mean instantaneous firing rate per condition. Note the high face-selectivity in both face conditions. **(B)** Movie experiment (six minutes fragment of "The Circus" film). Movie frames were binned into four different types of frames of the movie (i.e., large, medium, small, and no faces). Note the higher average firing rate for frames with large faces. Error bars denote standard error of mean (SEM).

## Supplementary References

1. Corlier, J., *et al.* Voluntary control of intracortical oscillations for reconfiguration of network activity. *Scientific Reports* **6**, 36255 (2016).
2. Chammat, M., *et al.* Cognitive dissonance resolution depends on episodic memory. *Scientific Reports* **7**, 41320 (2017).
3. El Karoui, I., *et al.* Event-related potential, time-frequency, and functional connectivity facets of local and global auditory novelty processing: an intracranial study in humans. *Cereb. Cortex* **25**, 4203-4212 (2014).
4. Babo-Rebelo, M., Wolpert, N., Adam, C., Hasboun, D. & Tallon-Baudry, C. Is the cardiac monitoring function related to the self in both the default network and right anterior insula? *Phil. Trans. R. Soc. B* **371**, 20160004 (2016).
5. Fried, I., *et al.* Cerebral microdialysis combined with single-neuron and electroencephalographic recording in neurosurgical patients. *J. Neurosurg.* **91**, 697-705 (1999).
6. Brainard, D.H. The Psychophysics Toolbox. *Spat. Vis.* **10**, 433-436 (1997).
7. Reddy, L., *et al.* Learning of anticipatory responses in single neurons of the human medial temporal lobe. *Nat. Commun.* **6** (2015).
8. Quiroga, R.Q., Reddy, L., Kreiman, G., Koch, C. & Fried, I. Invariant visual representation by single neurons in the human brain. *Nature* **435**, 1102-1107 (2005).
9. Kornblith, S., Quiroga, R.Q., Koch, C., Fried, I. & Mormann, F. Persistent single-neuron activity during working memory in the human medial temporal lobe. *Curr. Biol.* **27**, 1026-1032 (2017).
10. Quiroga, R.Q., Nadasdy, Z. & Ben-Shaul, Y. Unsupervised spike detection and sorting with wavelets and superparamagnetic clustering. *Neural Comput.* **16**, 1661-1687 (2004).
11. Blatt, M., Wiseman, S. & Domany, E. Superparamagnetic clustering of data. *Phys. Rev. Lett.* **76**, 3251 (1996).
12. Freiwald, W.A., Tsao, D.Y. & Livingstone, M.S. A face feature space in the macaque temporal lobe. *Nat. Neurosci.* **12**, 1187-1196 (2009).

13. Maris, E. & Oostenveld, R. Nonparametric statistical testing of EEG-and MEG-data. *J. Neurosci. Methods* **164**, 177-190 (2007).
14. Nir, Y., *et al.* Interhemispheric correlations of slow spontaneous neuronal fluctuations revealed in human sensory cortex. *Nat. Neurosci.* **11**, 1100-1108 (2008).
15. Self, M.W., *et al.* The effects of context and attention on spiking activity in human early visual cortex. *PLoS Biol.* **14**, e1002420 (2016).
16. Axelrod, V. & Yovel, G. Hierarchical Processing of Face Viewpoint in Human Visual Cortex. *J. Neurosci.* **32**, 2442-2452 (2012).
17. Axelrod, V., Rees, G. & Bar, M. The default network and the combination of cognitive processes that mediate self-generated thought. *Nature Human Behavior* **1**, 896-910 (2017).
18. Berman, M.G., *et al.* Evaluating functional localizers: The case of the FFA. *Neuroimage* **50**, 56-71 (2010).
19. Gilaie-Dotan, S. & Malach, R. Sub-exemplar Shape Tuning in Human Face-Related Areas. *Cereb. Cortex* **17**, 325-338 (2007).
20. Goesaert, E. & Op de Beeck, H.P. Representations of Facial Identity Information in the Ventral Visual Stream Investigated with Multivoxel Pattern Analyses. *J. Neurosci.* **33**, 8549-8558 (2013).
21. Smith, S.M., *et al.* Advances in functional and structural MR image analysis and implementation as FSL. *Neuroimage* **23**, S208-S219 (2004).
22. Rossion, B., Hanseeuw, B. & Dricot, L. Defining face perception areas in the human brain: a large-scale factorial fMRI face localizer analysis. *Brain Cogn.* **79**, 138-157 (2012).
23. Fox, C.J., Iaria, G. & Barton, J.J.S. Defining the face processing network: Optimization of the functional localizer in fMRI. *Hum. Brain Mapp.* **30**, 1637-1651 (2009).